

Encounter-triggered disc mass loss in the ONC

C. Olczak, S. Pfalzner

I. Physikalisches Institut, University of Cologne, Germany

R. Spurzem

Astronomisches Rechen-Institut, Zentrum für Astronomie, Univ. Heidelberg

ABSTRACT

The relevance of encounters on the destruction of protoplanetary discs in the Orion Nebula Cluster (ONC) is investigated by combining two different types of numerical simulation. First, star-cluster simulations are performed to model the stellar dynamics of the ONC, the results of which are used to investigate the frequency of encounters, the mass ratio and separation of the stars involved, and the eccentricity of the encounter orbits. The results show that interactions that could influence the star-surrounding disc are more frequent than previously assumed in the core of the ONC, the so-called Trapezium cluster. Second, a parameter study of star-disc encounters is performed to determine the upper limits of the mass loss of the discs in encounters. For simulation times of ~ 1 - 2 Myr (the likely age of the ONC) the results show that gravitational interaction might account for a significant disc mass loss in dense clusters. Disc destruction is dominated by encounters with high-mass stars, especially in the Trapezium cluster, where the fraction of discs destroyed due to stellar encounters can reach 10-15%. These estimates are in accord with observations of Lada et al. (2000) who determined a stellar disc fraction of 80-85%. Thus, it is shown that in the ONC - a typical star-forming region - stellar encounters do have a significant effect on the mass of protoplanetary discs and thus affect the formation of planetary systems.

Subject headings: clusters - accretion discs - circumstellar matter - ONC

1. Introduction

According to current knowledge planetary systems form from the accretion discs around young stars. These young stars are in most cases not isolated but are part of a cluster. It

is still an open question as to how far encounters with the surrounding stars of the cluster influence planet formation. The fact is that these discs disperse over time either by photo-evaporation, encounter-induced disc mass loss or some other means. Simple calculations seem to indicate that encounters do not play an important role. Nevertheless, Scally & Clarke (2001) found that a little less than a third of stars in the central core of the ONC would suffer an encounter within 100 AU, and thus, for a significant minority of stars in the Trapezium cluster, star disk encounters are of some importance. However, in order to quantify how many stars would be expected to lose most of their disc material, it is necessary to treat the disc mass loss - and its dependence on the mass of the perturbing object - in a more sophisticated way than was done by Scally & Clarke (2001).

Like Scally & Clarke (2001) the ONC is used as model cluster for the following reasons: The ONC is thought to be a typical environment for star-formation and its high density suggests that stellar encounters might be relevant for the evolution of circumstellar discs. In addition, it is one of the best-studied regions in our galaxy, so that observational constraints significantly reduce the modelling parameters.

1.1. Structure and Dynamics of the ONC

The ONC is a rich stellar cluster with about 4000 members with masses M^* above $0.08 M_\odot$ in a volume ~ 5 pc across (Hillenbrand & Hartmann 1998; Hillenbrand & Carpenter 2000). Most of the objects are T Tauri stars, but there is also strong evidence for the existence of several protostars. The mean stellar mass is about $0.5 M_\odot$ (Scally, Clarke & McCaughrean 2005), the half-mass radius roughly 1 pc. Recent studies on the stellar mass distribution (Hillenbrand & Carpenter 2000; Luhman et al. 2000; Muench et al. 2002; Slesnick, Hillenbrand & Carpenter 2004) reveal no significant deviation from the field star IMF Kroupa, Tout & Gilmore (1993)

$$\xi(M^*) = \begin{cases} 0.035 M^{*-1.3} & \text{if } 0.08 \leq M^* < 0.5, \\ 0.019 M^{*-2.2} & \text{if } 0.5 \leq M^* < 1.0, \\ 0.019 M^{*-2.7} & \text{if } 1.0 \leq M^* < \infty. \end{cases} \quad (1)$$

The shape of the system is not perfectly spherical but elongated in the north-south direction. The reason for this asymmetry is the gravitational potential of a massive molecular ridge in the background of the cluster, OMC 1, being part of the much larger complex of the Orion Molecular Cloud. The mean age of the whole cluster has been estimated to be about 1-2 Myr, though with a significant age spread of the individual stars. Today, star formation is no longer occurring in the cluster itself, only in the background molecular cloud. After

a short period of intense star-formation the ONC has expelled most of the residual gas by now.

The density and velocity distribution of the ONC resembles an isothermal sphere. From the outer edge the number of stars falls linearly with decreasing radius r down to ~ 0.1 pc; inside this cluster core, the distribution function becomes flatter (Jones & Walker 1988; McCaughrean & Stauffer 1994; Hillenbrand 1997; Hillenbrand & Hartmann 1998; McCaughrean et al. 2002). The central number density ρ_{core} in the inner 0.053 pc reaches $4.7 \times 10^4 \text{ pc}^{-3}$ (McCaughrean & Stauffer 1994) and makes the ONC one of the densest star forming regions in the Galaxy. The velocity dispersion is nearly constant for all cluster radii. In their proper motion study of the ONC, Jones & Walker (1988) have obtained a three-dimensional velocity dispersion of 4.3 km s^{-1} , thus the crossing time is $t_{\text{cross}} = 2R_{\text{hm}}/\sigma \approx 0.5$ Myr. Another crucial quantity in stellar dynamics is the virial ratio Q_{vir} , which has been estimated for the ONC as

$$Q_{\text{vir}} = \frac{R_{\text{hm}}\sigma^2}{2GM} \approx 1.5, \quad (2)$$

where R_{hm} is its half-mass radius. This indicates that the ONC is not only far from virial equilibrium, but even seems to be gravitationally unbound ($Q_{\text{vir}} > 1$). However, this statement has to be treated with care because errors in the observational parameters can easily account for an error of over 50 per cent in this calculation. Besides, the estimated total mass of the ONC of $2000 M_{\odot}$ is only a lower limit since a substantial amount could be present in undetected low-mass binary companions or gas. Furthermore, the contribution of the OMC 1 to the overall gravitational potential is still unknown and the elongated shape of the cluster indicates that it is not negligible. However, as long as measurements of velocities and masses lack higher precision, one cannot constrain the cluster dynamics to contraction, equilibrium or expansion.

Like many other stellar aggregations, the ONC shows mass segregation, with the most massive stars being confined to the inner cluster parts. The Trapezium cluster, a subgroup of about 1000 stars in a volume 0.6 pc across, represents the denser core of the Orion Nebula Cluster. It contains four luminous O and B stars at the very center, designated as the Trapezium. Their most prominent member, $\theta^1\text{C Ori}$, is a O6 star with a mass of about $50 M_{\odot}$, a luminosity of $4 \times 10^5 L_{\odot}$ and a surface temperature of $4 \times 10^4 \text{ K}$.

Apart from its high density and young age, the evidence for protoplanetary discs around many stars in this cluster makes the ONC the ideal candidate for the present investigation. Whereas the first identification of “peculiar stellar objects” dates back to the paper from Laques & Vidal (1979), it took more than a decade to recognize them as circumstellar discs which are ionized by the intense radiation of the Trapezium stars. O’Dell, Wen & Hu (1993)

designated these bright objects as “proplyds”. At greater distances from the cluster centre they also detected their dark counterparts: discs in silhouette which are visible due to the bright nebular background. Thus far, about 200 bright proplyds and 15 silhouette discs have been revealed in several HST studies of the ONC (O’Dell, Wen & Hu 1993; O’Dell & Wong 1996; Bally et al. 1998; Bally, O’Dell & McCaughrean 2000), nearly all located in the Trapezium cluster due to selection effects.

The most recent study on circumstellar discs in the Trapezium (Lada et al. 2000) used the L-band excess as detection criterium. They analyze 391 stars and find a fraction of 80-85% to be surrounded by discs. This is in agreement with an earlier investigation of the larger ONC in which Hillenbrand (1997) states a disc fraction of 50-90%. The disc sizes established so far vary between 50 AU and 1000 AU, with a typical value of 200 AU for low-mass stars. The inferred disc masses are only accurate to an order of magnitude but seem not to exceed a few percent of the central stellar mass, which classifies them as low-mass discs. The disc surface densities are generally well described by power-law profiles, $\Sigma(r) \propto r^{-a}$, with $0.5 \leq a \leq 1.5$.

1.2. Previous work

At present it is not possible to perform numerical particle simulations where the stars including their surrounding discs are sufficiently resolved to determine the effect of encounters on the discs quantitatively. Therefore Scally & Clarke (2001) treated the dynamics of the stars in the cluster and star-disc encounters and photoevaporation effects in separate investigations and combined the results to determine the disc destruction rate. The term star-disc encounters means here encounters where only one of the stars is surrounded by a disc, in contrast to disc-disc encounters denominating encounters where both stars are surrounded by discs.

In order to determine the disc destruction rate a number of assumptions were made by Scally & Clarke (2001):

1. The discs around the stars do not alter the stellar dynamics in any significant way.
2. The discs are of low mass.
3. Only two stars are involved in an encounter event and three-(or even more) body events are so rare that they can be neglected.
4. The encounters were modelled as coplanar and prograde.

5. The disc mass loss is deduced from parameter studies of star-disc encounters.
6. The closest encounter is the most destructive one.
7. A parameter study of encounters between equal mass stars is used.

From the last point Scally & Clarke (2001) concluded that only in penetrating encounters a significant amount of mass can be stripped from the disc. Assuming a typical disc size of 200 AU, they considered the stars with separations of less than 100 AU. Under these assumptions Scally & Clarke (2001) found that just 3-4% of all discs have the potential to be destroyed by encounters.

1.3. Aim and structure of present work

In this work we concentrate on the effect of encounters on the disc dispersal and ignore photo-evaporation. We performed an investigation similar to that of Scally & Clarke (2001) but drop the last two assumptions of above list. In contrast to Scally & Clarke (2001) i) we record the entire path history of each star, so the effect of repeated encounters is included, ii) extend the parameter study to include encounters with massive perturbers and iii) record the most forceful encounter. It will be demonstrated that these modifications alter significantly the result, so that the conclusion that encounters can be excluded as a disc destruction mechanism should be revised.

The paper is organized the following way: In Section 2 we begin with simulations of the ONC. This is followed by an investigation of the mass loss in star-disc encounters in Section 3, resulting in a fitting formula for the disc mass loss. In Section 4 the results of Section 2 and 3 are combined to determine the disc dispersal as a function of time. In Section 5 it will be discussed how the disc mass loss is influenced by the assumptions made.

2. Cluster Simulations

2.1. Initial conditions

The dynamical models of the ONC presented here contain only pure stellar components without considering gas or the potential of the background molecular cloud OMC 1. All cluster models were set up with a spherical density distribution $\rho(r) \propto r^{-2}$ and a Maxwell-Boltzmann isotropic velocity distribution. The masses were generated randomly according

to the mass function given by Eq. (1) in a range $50 M_{\odot} \geq M^* \geq 0.08 M_{\odot}$ apart from the most massive star, representing $\theta^1\text{C Ori}$, which was directly assigned a mass of $50 M_{\odot}$, as in a random mass generation process only in very few cases the highest mass exceeds $30 M_{\odot}$. $\theta^1\text{C Ori}$ was placed at the cluster centre and the other three Trapezium members were assigned random positions in a sphere of $0.3R_{\text{hm}}$. This procedure accounts for the initial mass segregation which is observed in young clusters and follows the study of Bonnell & Davies (1998). Except for the positioning of these three stars and the separate generation of $\theta^1\text{C Ori}$, this configuration is identical to the setup of Scally & Clarke (2001).

The ONC was simulated for a total time of 13 Myr, which is the assumed lifetime of $\theta^1\text{C Ori}$. The quality of the dynamical models was determined by comparison to the observational data after a simulation time of 1-2 Myr, which marks the range for the mean age of the ONC. The quantities of interest were the number of stars, the half-mass radius, the number densities, the velocity dispersion and the projected density profile.

The virial ratio Q_{vir} of the cluster is a crucial quantity for its dynamics. Contracting models ($0.01 \leq Q_{\text{vir}} < 0.5$) showed only moderate agreement with observations in the density distribution and only after at least 2 Myr simulation time. However, this scenario was not excluded for the study since the age spread of the ONC is large and star formation set in more than 4 Myr ago. Unbound models with $Q_{\text{vir}} > 1.0$ were not further considered since unreasonable high initial core densities of $\rho_{\text{core}} > 10^6 \text{ pc}^{-3}$ are required in this case and the resulting density distribution did not resemble the observations very well. Hence, only models with $0.01 \leq Q_{\text{vir}} \leq 1.0$ are presented here. This constraint is also in accordance with the recent results from Scally, Clarke & McCaughrean (2005).

Three configurations, A, B and C, were chosen as the best dynamical models of the ONC, according to $Q_{\text{vir}} = 0.5$, $Q_{\text{vir}} = 1.0$ and $Q_{\text{vir}} = 0.1$, respectively. The parameters of the three configurations are summarized in Table 2. Ten random setups of each of these initial models were simulated to minimize statistical variations in the results.

2.2. Numerical method

The cluster simulations were performed with NBODY6++ (Spurzem & Baumgardt 2002), which allows a high-accuracy treatment of two-body interactions and is a parallelized version of NBODY6 (Aarseth 2003). Since the aim of this work was to record the encounters in the ONC, additional routines had to be implemented:

Apart from storing the closest encounter for each star a more advanced encounter list was produced: The search criterion for the next perturber of a star was modified by considering

the gravitationally most dominating body instead of the closest neighbour, or in other words, the minimization of the distance was replaced by the maximization of the gravitational force. The former scheme underestimates the effect of stellar encounters since the nearest neighbour is not necessarily the gravitationally dominant one. Approaches of stars were only considered to be true encounters if the orbit of the perturber was concave and if the calculated relative disc mass loss was higher than the 1σ error, which is 0.03 in this study.

As the above approach would only account for one single encounter for every star, the encounter list was extended by recording the information of *all* perturbing events of each stellar disc during the course of the simulation. In order to obtain the disc mass loss, both masses, the relative velocity and the eccentricity were additionally recorded, which constitute the full set of orbital parameters determining the planar two-body problem.

2.3. Cluster results

Here we will mainly describe the results from the model in virial equilibrium (A) and discuss the expanding and contracting model in Section 4. In Fig. 1 the temporal development of the total particle number and the number of particles confined to the volume of the ONC and the Trapezium, are shown. The total particle number in the simulation decreases because particles reaching the numerical cutoff radius ($\sim 20R_{\text{hm}}$) are excluded from the simulation. The particle number in the entire simulation volume is nearly unchanged for the whole simulation time of 13 Myr, only 4% of all particles exceeded the cutoff radius. If one considers the ONC volume, the population is reduced slightly more, but only for simulation times larger than 2 Myr, marked by the right vertical dotted line. Still 95% of the initial number is preserved and thus satisfies the observational constraints. In the Trapezium volume, the population initially rises, which means that the inner core of the cluster undergoes some contraction. After approximately 0.5 Myr this trend is inverted, reducing the stellar number to nearly 1000 or 800 after 1 Myr or 2 Myr, respectively. This behaviour is also reflected in the time-dependence of the half-mass radius on the right-hand axis, which decreases from 0.55 pc to 0.46 pc at its minimum.

The rise of the virial ratio at the beginning of the simulation is mainly due to the gain of potential energy by contraction of the cluster, which results in a rise of the kinetic energy by an equal amount due to energy conservation. The heating of the entire core finally overcomes the gravitational drag and inverts the inward motion of the stars; the fastest of these soon leaving the boundary of the ONC. After several crossing times the system begins to relax and the virial ratio is roughly constant, $Q_{\text{vir}} = 0.6$, which means that the cluster is still a bound entity.

In Fig. 2 the density profile of the model cluster A at 1 Myr and 2 Myr is compared to data from infrared observations performed by McCaughrean et al. (2002). Both curves fit well up to a distance of 0.3 pc, and therefore qualify as a model for the ONC. For larger distances the values are somewhat below the observed profile. This is due to the initially truncated particle distribution and evaporation of the system. However, since this investigation focuses on the effect of encounters on the disc mass in the inner Trapezium cluster, this should not significantly influence the results.

As mentioned before one main reference was the work of Scally & Clarke (2001) who found stellar encounters to play only a minor role even in such a dense environment. The initial conditions of their model (designated as model A*) are identical to model A with the exception of a nearly two times larger initial extension. As Fig. 3 shows, choosing an analogous cluster setup, the distribution of closest encounters presented in Scally & Clarke (2001) could be reproduced very well. Fig. 3 presents two histograms of r_{close} for all the stars in the cluster after a simulation time of 2.9 Myr and 12.5 Myr, respectively, with r_{close} for each star representing its overall minimum separation to any other object in the cluster - this quantity can only either remain constant or decrease with time. At a simulation time of 2.9 Myr only few ($\sim 4\%$) very close encounters with a separation of less than 100 AU have occurred, while the majority of stars never approached closer than 1000 AU and even after 12.5 Myr only slightly more than 5% of the stars were encountered closer than 100 AU.

While the shape of the projected density profile shown in Fig. 2 provides a reasonable fit to the observational data, the magnitude of the density in the inner cluster parts is nearly two times lower (thus the density profile had to be shifted upwards in figure 2 for comparison with the VLT data). So that we conclude that model A provides a better fit to the observational data and will apply it in the analysis that follows.

Fig. 4 demonstrates that for model A the median is far below 1000 AU, after 12.5 Myr it even approaches 500 AU. This shifting directly reflects the roughly two times higher initial density of model A. Analogously, the number of stars with r_{close} lower than 100 AU more than doubles resulting in a fraction of 9.4% for 2.9 Myr and 11.9% after 12.5 Myr.

2.4. Mass Loss

Combining the results of Section 2 and 3, the relative disc mass loss for each disc is obtained as a function of the simulation time. The parameters of each stellar encounter were taken from the stellar encounter lists generated by preprocessing the original encounter list of each single run. The calculation of the disc mass loss due to encounters was performed

for each single run and then averaged over ten simulations.

According to the improved fit function (??), the relative mass loss of a stellar disc was obtained from the perturber periastron. For this purpose, first the disc size of the central star was scaled due to the stellar mass by using Eq. (??), then the relative perturber mass, M_2^*/M_1^* , and the relative periastron, r_p/r_d were passed to the fit function (??). The errors of the estimated relative disc mass loss due to each encounter i , $\Delta^i = \Delta^i(r_p/r_d)$, were assumed to be $\Delta^i = 0.03$ for $r_p/r_d > 1$, $\Delta^i = 0.05$ for $r_p/r_d > 0.1$ and $\Delta^i = 0.1$ if $r_p/r_d = 0.1$, according to the statistical errors of the encounter simulations.

In the following it will be shown for our model A that an improved encounter treatment is important because (a) the majority of the stars in the model clusters undergo more than one encounter, (b) a large fraction of the stars encounter a much more massive perturber, and (c) the largest perturbation of a disc is caused by the gravitationally most dominating body and **not** by the closest companion.

Defining an encounter as a perturbing event in which a circumstellar disc loses at least 3% of its mass, Fig. 6 shows that the effect of (c) for the number of perturbed discs is only minor. In contrast, the improvement (a) has a much larger effect: roughly half of all discs that have been perturbed have been done so repeatedly. Thus, a realistic investigation of stellar encounters in young clusters and their effect on protoplanetary discs cannot be performed without considering the entire encounter history of each star.

In Fig. 7 the effect of (b) and (c) is shown by plotting the ratio of the perturber mass M_2^* and that of the encountered star M_1^* , $M_2^*/M_1^* = 2$ and $M_2^*/M_1^* = 10$, for the two encounter criteria, respectively. If this quantity is significantly higher than unity, then even non-penetrating stellar encounters have the potential to remove a large fraction of a disc's mass. In contrast to Fig. 6 it is apparent that (c) has a major effect: this criterion causes a twice as large number of high mass ratios in both cases, $M_2^*/M_1^* = 2$ and $M_2^*/M_1^* = 10$, when comparing the strongest and the closest perturber. This means that while the number of perturbed discs does not change significantly, the effect of (c) on the disc mass loss is large. The effect of (b) is given by comparing the numbers with Fig. 6. It is evident that most perturbed discs have been approached by a companion at least twice as massive as the central star, and nearly half of them was more than ten times heavier. Again, this improvement of the treatment of encounters has a strong impact on the disc mass loss.

For the clusters in virial equilibrium (Model A), Fig. 8 depicts the distribution of the relative disc mass at different simulation times in a histogram exemplary for an intermediate standard disc size, $r_{sd} = r_d(1 M_\odot) = 150 \text{ AU}$. Each plot contains two distributions, one in which the entire encounter history of all stars in the cluster was considered, and the

other accounting only for the closest encounter. It is apparent from the plots that both distributions have a prominent minimum near relative disc masses of 0.5, which means that shortly after the simulation start the stellar population divides roughly into two groups, one containing the stars which have virtually undisturbed discs and the other those which have lost the major part of their disc. The former diminishes from roughly 95% at 0.1 Myr and to 72% at 13 Myr. There are in general only slight differences between the two distributions of Fig. 8 if one neglects the leftmost bin, which means that as long as the relative disc mass does not fall below 5%, the closest encounter of each star determines entirely its disc mass loss, independent of eventual additional encounters.

The situation is very different if one considers only the stars with at least a disc mass loss above 95%. There are roughly six times more stars when one models repeated and high M_2^*/M_1^* encounters, more precisely 1.5% instead of 0.25% at 0.1 Myr, and 4.9% instead of 0.8% at 13 Myr, respectively. So only a sequence of several encounters has the potential to completely disrupt a significant number of protoplanetary discs. Hence, the encounter scenario used in this work decisively affects the statistics on the disc mass loss due to encounters, particularly for the extreme case of a nearly total removal of a star’s disc material.

In the second realization of the distribution of the relative disc mass, shown in Fig. 9, the histograms are plotted for two different standard disc sizes, 100 AU and 200 AU, at 1 Myr simulation time. It is apparent that in accordance with the doubled size of the standard disc size the disc mass loss is far higher. This finding demonstrates the sensitivity of the disc mass loss on the choice of the standard disc size r_{sd} , the relation of which to the disc size r_d is given by Eq. (??), and thus justifies its application as a free parameter as well in Fig. 10.

Here, the fraction of still un-destroyed discs is plotted against simulation time for the same two standard disc sizes r_{sd} . The plot in Fig. 10 depicts the fraction of un-destroyed discs for the entire ONC and for the Trapezium cluster. The dotted horizontal line represents the upper limit of the fraction of disc surrounded stars in the Trapezium of 80-85% (Lada et al. 2000). It is apparent that the period of most violent disc destruction lasts for roughly 2 Myr after the simulation start, consistent with the phase of slight contraction of model A.

Equally, the doubled standard disc size affects the fraction of un-destroyed discs directly in the sense that the fraction of *destroyed* discs becomes two times higher.

A comparison of the resulting fraction of remaining discs in the Trapezium with the observational estimates of Lada et al. (2000) shows that the upper limit of 85% is not surpassed in the specified range of the ONC’s mean age. This is interpreted as a correspondence with observations since it is likely that processes other than star-disc encounters, e.g. photo-evaporation (Scally & Clarke 2001), do account for the destruction of protoplanetary discs

and thus the fraction of remaining discs due to encounters alone should be higher than the observational value. Moreover, the observational estimates state perhaps even lower limits since it is much more likely to fail with the detection of circumstellar discs due to sensitivity limits than to classify a bare star as a star-disc system. However, with increasing time the fraction of remaining discs decreases further and reaches nearly an asymptotical value at the end of the simulation which implies that star-disc encounters in a dense core like the Trapezium could even destroy up to 20% of all discs.

Considering now an expanding (model B) and contracting (model C) cluster, our simulations show that for the expanding model in the Trapezium cluster the fraction of remaining discs rises much faster due to the twice as high initial core density. However, the period of violent interaction is much shorter due to the fast expansion and so that again the fraction of un-destroyed discs is 85-95% in the Trapezium but this level is already reached at 0.5 Myr. However, in the case of the entire ONC, the fraction of remaining discs stays much higher than in model A as here the fast expansion of the outer regions is not compensated by a highly increased density, which is required for close interactions of objects with high velocities.

In the contracting model the fraction of destroyed discs in the entire ONC is fairly low for all times. For the Trapezium cluster the population grows faster than discs are destroyed so that the relative number of destroyed discs actually decreases. If the ONC was initially in a dynamically cold state, so that 90-95% of the discs in the Trapezium cluster would not have been seriously disrupted and the effect of star-disc encounter on the disc mass loss of protoplanetary discs would be negligible in the case of a contracting cluster.

3. Discussion

In the previous sections it was repeatedly stated that the results here represent an upper limit for the destruction of discs by encounters in the ONC. In the following this will be explained in more detail and estimates for lower limits of the mass loss given.

The situation described above contains, like previous work, a contradiction - it was assumed that each star is initially surrounded by a disc and at the same time the disc mass loss that a star (without disc) produces in a star disc system was considered. Logically both stars would have to be surrounded by a disc each. There are two reasons why this was done. First, encounters where both stars are surrounded by discs are less well investigated and second Pfalzner et al. (2005b) showed that the star-disc results can be generalized to disc-disc encounters as long as there is no mass exchange between the discs. In the case of

a mass exchange the discs can be to some extent replenished so that the mass loss would be overestimated.

Eq. (??) is valid for parabolic encounters. Binary formation ($\epsilon < 1$) can be neglected as in this study it happens in less than 0.5% of all encounters. However, most encounters in the cluster simulations are not parabolic but hyperbolic. In such hyperbolic encounters the mass loss is lower because the disturber is not long enough in the vicinity of the star-disc system to remove disc mass. However, considering only the stars that lose more than 90% of their disc mass, the eccentricity ϵ of their orbits has a maximum at $\epsilon \approx 3$ (see Fig. 11). Pfalzner et al. (2005a) showed that for $M_2^* = 1 M_\odot$ the relative disc mass loss in an $\epsilon = 3$ encounter is about 55% of that of a parabolic encounter.

It is still an open question whether discs in clusters are in any way aligned and whether there is a preference for coplanar or prograde encounters due to the common formation history of the involved stars and discs. If the coplanar, prograde encounters considered here are in any way favoured, they are the most destructive type of encounter. However, in a cluster that is not highly flattened it seems rather unlikely that the encounter planes are to a high degree aligned. Therefore one would expect most encounters to be noncoplanar. Pfalzner et al. (2005a) showed that, as long as the inclination is not larger than 45° the mass loss in the encounter is only slightly reduced in comparison to a coplanar encounter. If however the orientation is completely random and a 90° -encounter the most likely encounter scenario, the mass loss could be significantly reduced. This point needs further investigation.

In this investigation it was assumed that in repeated encounters the relative mass loss is the same. This is somewhat in contrast to the prevailing view that an encounter ‘hardens’ a disc so that later encounters can no longer influence it. This effect of disc hardening might happen for high-mass discs but for low-mass discs Pfalzner (2004) found that although the total disc mass loss was smaller in a second encounter the relative disc mass loss was the same as in the first encounter. As this has only been tested in a particular case ($M_2^* = 1 M_\odot$), it should be investigated whether this holds generally. It is important to note that the calculations of Pfalzner (2004) are ballistic particle simulations, neglecting the effects of viscosity. Simulations of star-disc encounters by Clarke & Pringle (1993) have shown that in this case discs get puffed up by encounters. On the other hand, the inclusion of dissipation lead to recircularisation of the remnant disc and hence disc shrinkage. Thus one might conclude that disc hardening must be underestimated by Pfalzner (2004). However, Pfalzner et al. (2005b) have as well investigated the effect of viscosity on different disc parameters and found no significant differences neither in the mass loss nor in the density distribution.

In this study it was assumed that all encounters can be described as two-body processes. Umbreit (2005) found from three-body encounters simulations that the resulting discs are

flatter and less massive than after similar two-body encounters with the same minimum encounter distance.

In this work it has not been considered that a considerable proportion of the stars in the ONC are not single stars but binary systems. Further studies would be needed to see if binary systems would lead to a different disc destruction rate. A second point for future investigations would be the inclusion of gas in the ONC simulations.

One should as well emphasize that the disc mass loss falls below 10% for mass ratios below 0.1, so the contribution from light perturbers is negligible as long as they are not penetrating the disc. Regarding the setup of the cluster simulations, the cut-off in the cluster IMF at substellar masses ($M^* \leq 0.08 M_\odot$) should thus have only a minor effect on the cumulative disc mass loss.

4. Conclusion

This investigation for the ONC cluster, combining cluster simulations with encounter investigations, shows that potentially up to 10-15% of the discs in the Trapezium cluster could have been destroyed by encounters. Our more sophisticated treatment of disc mass loss expected from multiple stellar encounters implies that it is plausible that the 15-20% of discless stars observed in the Trapezium (Lada et al. 2000) may, in a large fraction of cases, result from star-disc collisions.

One important result is that the most massive bodies dominate the disc mass loss, with significant interaction even beyond a separation of ten disc radii for a ONC-like entity. This is particularly so for the Trapezium, where some dozen massive stars are surrounded by hundreds of lighter bodies. Consequently, it is the upper end of a cluster’s mass distribution that to a large degree determines the fate of the circumstellar discs in its vicinity and thus there are in principle two quantities that are mainly regulating the effect of stellar encounters on the mass-loss from protoplanetary discs: namely the local stellar density which determines the encounter probability, and the upper limit of the mass range, which affects the maximum strength of the perturbing force.

As the number of massive members in a stellar group seems to be correlated to its initial density (see Testi et al. 1997; Bonnell et al. 2004) and the IMF appears to be uniform for all Galactic environments (e.g Kroupa, Tout & Gilmore 1993; Muench et al. 2000) of star-formation, the dependency of the disc mass loss due to encounters is mainly reduced to one parameter, namely the density distribution of the considered stellar system. This relation would be worth investigating in future.

As the possible disc destruction rate is so high, it is obvious that the remaining discs are considerably affected by encounters - that is the mass distribution and the cut-off radius of the disc. These properties are two ingredients vital for the understanding of the formation of planetary systems. Further studies of the temporal evolution of these properties in the ONC are on the way.

Acknowledgments

Simulations were partly performed at the John von Neumann Institut for Computing, Research Center Jülich, Project HKU14. We want to thank the referee C. Clarke for her very useful comments. RS wants to thank Sverre Aarseth for a sustained friendly and indispensable collaboration over many a project and code.

REFERENCES

- Aarseth, S. *Gravitational N-Body Simulations* 2003, CUP, Cambridge.
- Bally, J., Sutherland, R. S., Devine, D., Johnstone, D. 1998, AJ, 116, 293.
- Bally, J., Testi, L., Sargent, A., Carlstrom, J. 1998, AJ, 116, 854.
- Bally, J., O'Dell, C. R., McCaughrean, M. J. 2000, AJ, 119, 2919.
- Bonnell, I.A., Davies, M.B. 1998, MNRAS, 295, 691.
- Bonnell, I. A., Vine, S. G., Bate, M. R. 2004, MNRAS, 349, 735.
- Clarke, C. J., Pringle, J. E. 1993, MNRAS, 261 190.
- Haisch, K. E., Lada, E. A., Lada, C. J. 2001, ApJ, 553, 153.
- Hall, S. M., Clarke, C. J., Pringle, J. E. 1996, MNRAS, 278, 303.
- Heller, C. H. 1993, ApJ, 408, 337.
- Heller, C. H. 1995, ApJ, 455, 252.
- Hillenbrand, L. A. 1997, AJ, 113, 1733.
- Hillenbrand, L. A., Strom, S. E., Calvet, N., Merrill, K. M., Gatley, I., Makidon, R. B., Meyer, R. M., Skrutskie, M. F. 1998, AJ, 116, 1816.

- Hillenbrand, L. A., Hartmann, L. W. 1998, ApJ, 492, 540.
- Hillenbrand, L. A., Carpenter, J. M. 2000, ApJ, 540, 236.
- Jones, B. F., Walker, M. F. 1998, AJ, 95, 1755.
- Kroupa, P., Tout, C.A., Gilmore, G. 1993, MNRAS, 262, 545.
- Lada, C. J., Muench, A. A., Haisch, K. E., Lada, E. A., Alves, J. F., Tollestrup, E. V., Willner, S. P. 2000, AJ, 120, 3162.
- Laques, P., Vidal, J. L. 1979, A&A, 73, 97.
- Luhman, K. L., Rieke, G. H., Young, E. T., Cotera, A. S., Chen, H., Rieke, M. J., Schneider, G., Thompson, R. I. 2000, ApJ, 540, 1016.
- McCaughrean, M. J., Stauffer, J. R. 1994, AJ, 108, 1382.
- McCaughrean, M. J., O'Dell, C. R. 1996, AJ, 111, 1977.
- McCaughrean, M., Zinnecker, H., Andersen, M., Meeus, G., Lodieu, N. 2002, The Messenger, 109, 28.
- Muench, A. A., Lada, E. A., Lada, C. J. 2000, ApJ, 533, 358.
- Muench, A. A., Lada, E. A., Lada, C. J., Alves, J. 2002, ApJ, 573, 366.
- O'Dell, C. R., Wen, Z., Hu, X. 1993, ApJ, 410, 696.
- O'Dell, C. R., Wong, K. 1996, AJ, 111, 846.
- Ostriker, E.C. 1994, ApJ, 424, 292.
- Palla, F., Randich, S., Flaccomio, E., Pallavicini, R. 2005, ApJ, 626, L49.
- Pfalzner, S., Vogel, P., Scharwächter, J., Olczak, C. 2005, A&A, 437, 976.
- Pfalzner, S., Umbreit, S., Henning, Th. 2005, ApJ, 629, 526.
- Pfalzner, S. 2004, ApJ, 602, 356.
- Scally, A., Clarke, C. 2001, MNRAS, 325, 449.
- Scally, A., McCaughrean, M.J., Clarke, C. 2005, MNRAS, 358, 742.
- Slesnick, C. L., Hillenbrand, L. A., Carpenter, J. M. 2004, ApJ, 610, 1045.

- Spurzem, R., Baumgardt, H. 2002, MNRAS, submitted.
- Testi, L., Palla, F., Prusti, T., Natta, A., Maltagliati, S. 1997, A&A, 320, 159.
- Umbreit, S. 2001, Diploma thesis (University of Jena, Germany).
- Umbreit, S. 2005, PhD thesis (University of Heidelberg, Germany).
- van Altena, W. F., Lee, J. T., Lee, J.-F., Lu, P. K., Upgren, A. R. 1998, AJ, 95, 1744.
- Vicente, S. M., Alves, J. 2005, A&A, 441 195.
- Wen, Z., O’Dell, C. R. 1995, ApJ, 438, 784.

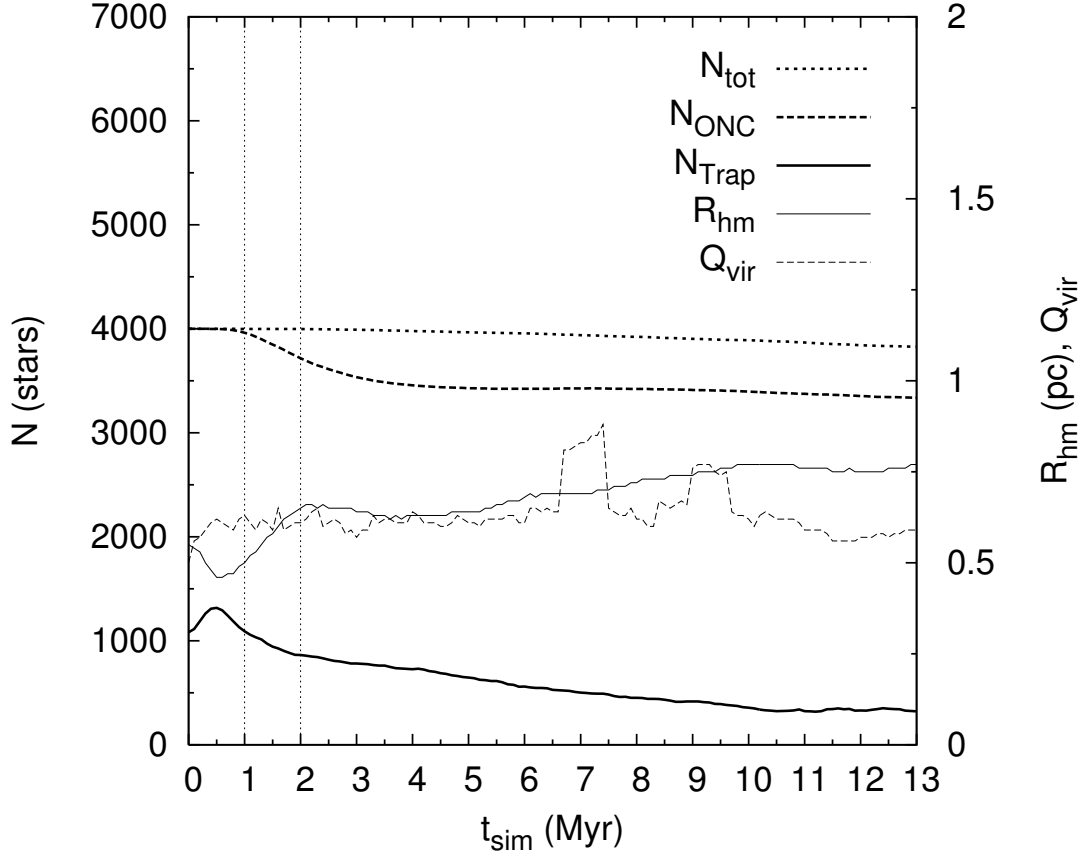


Fig. 1.— Time evolution of particle numbers, half-mass radius and virial ratio of the model cluster A. The particle numbers represent the total population, N_{tot} , the population of the ONC ($R_{\text{ONC}} = 2.5 \text{ pc}$), N_{ONC} , and that of the Trapezium cluster ($R_{\text{Trap}} = 0.3 \text{ pc}$), N_{Trap} , respectively.

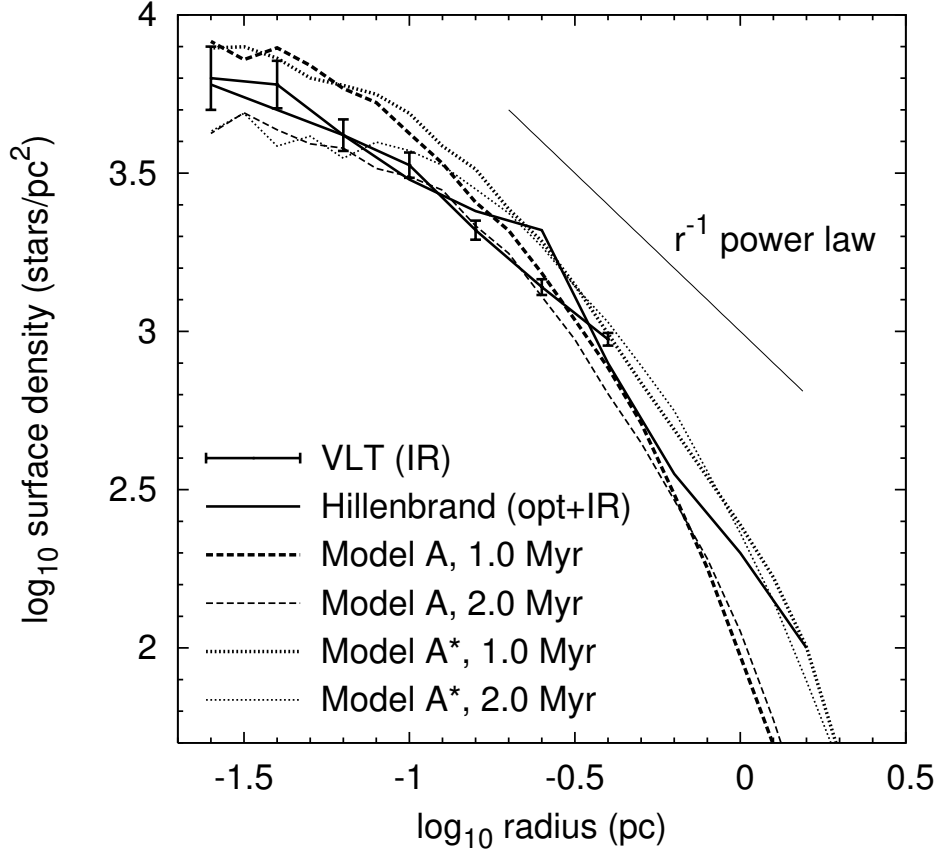


Fig. 2.— The density profile of the model cluster A at $t_{\text{sim}} = 1 \text{ Myr}$ and $t_{\text{sim}} = 2 \text{ Myr}$ is compared to data from infrared observations performed by McCaughrean et al. (2002) with the VLT. The original figure is from Scally, Clarke & McCaughrean (2005) and includes two additional data sets from Jones & Walker (1988) and Hillenbrand (1997). The set according to Jones & Walker (1988) has been excluded from this image for greater clearness. For comparison a power law of slope -1 is shown, corresponding to r^{-2} in three dimensions, the estimated profile of the ONC. The equivalent distributions for the simulations by Scally & Clarke (2001) are denoted as model A*. Here, due to the lower density of model A* by a factor of two, the distributions were shifted by the same factor to allow for comparison.

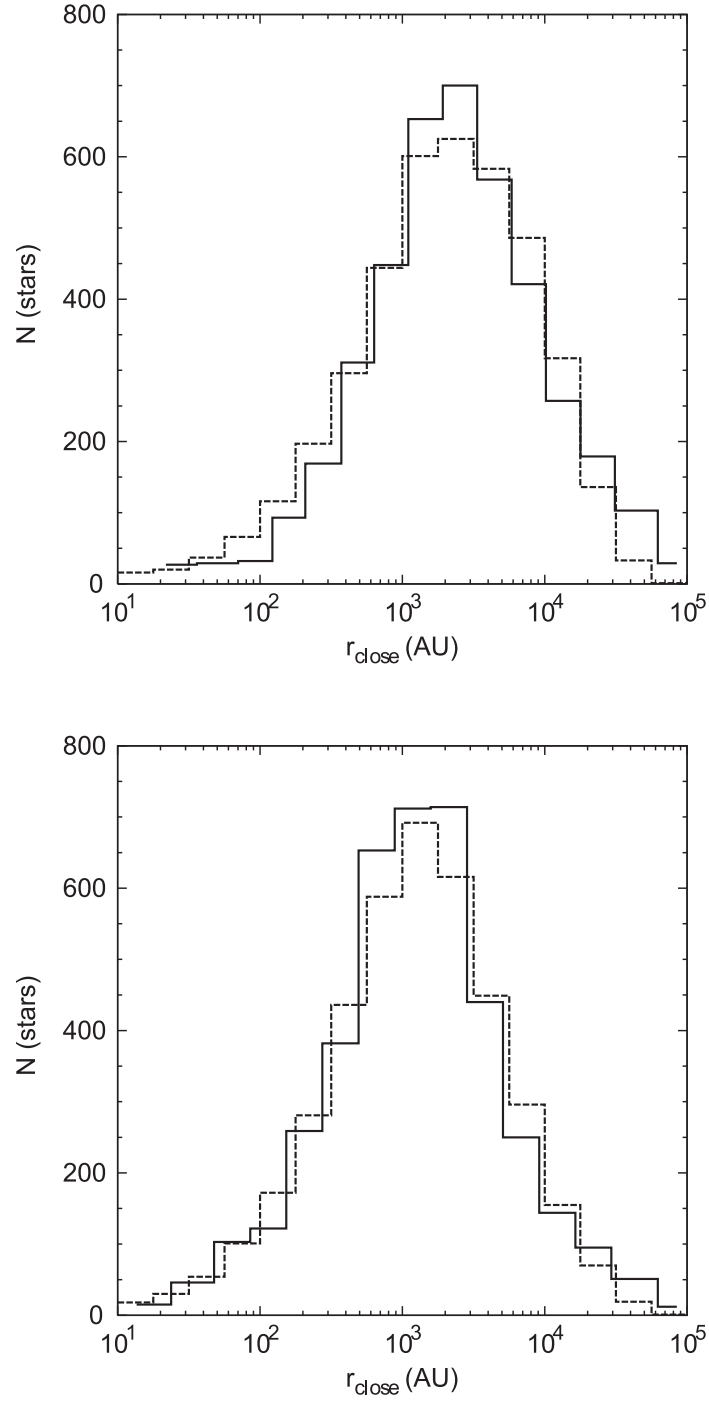


Fig. 3.— Number of stars as a function of the closest encounter distance. Comparison of model A* (dashed lines) with that of Scally & Clarke (2001) (drawn lines) at a) $t_{\text{sim}} = 2.9$ Myr and b) $t_{\text{sim}} = 12.5$ Myr.

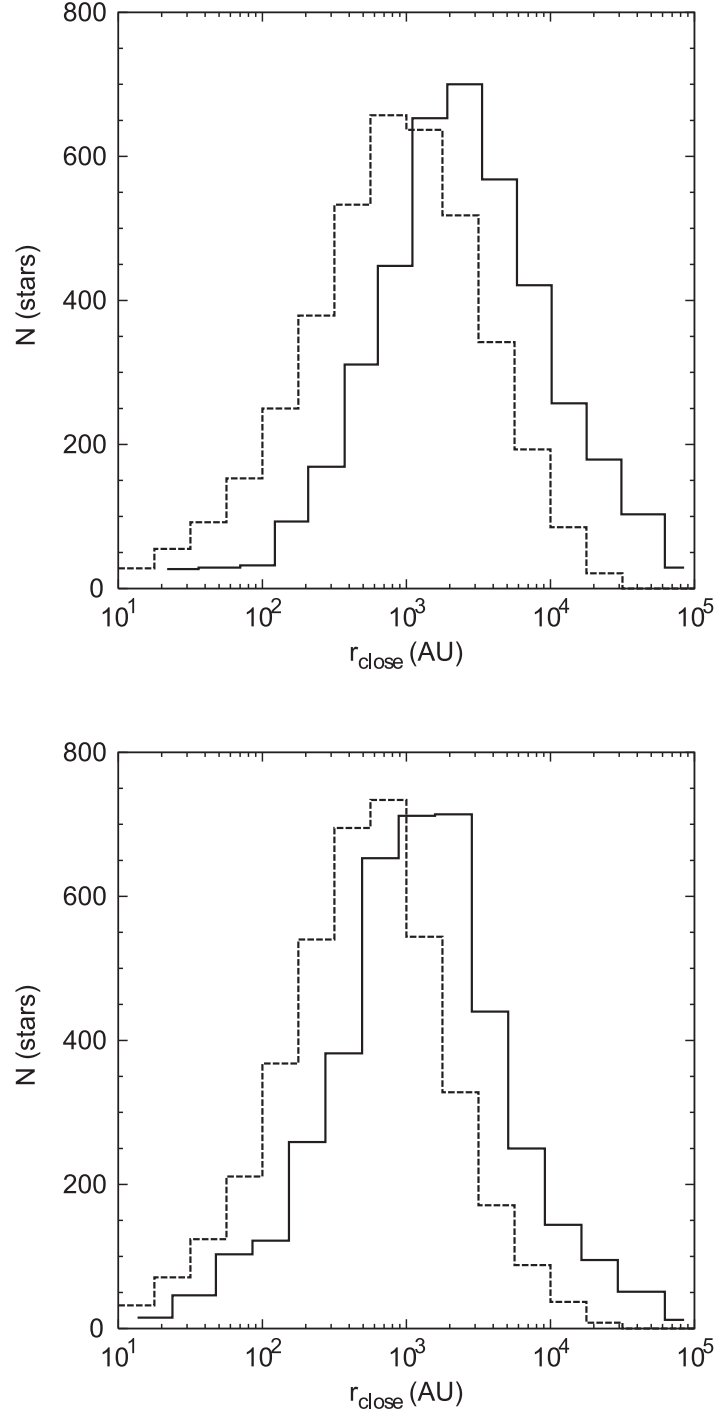


Fig. 4.— Number of stars as a function of the closest encounter distance. Comparison of model A (dashed lines) with that of Scally & Clarke (2001) (drawn lines) at a) $t_{\text{sim}} = 2.9 \text{ Myr}$ and b) $t_{\text{sim}} = 12.5 \text{ Myr}$.

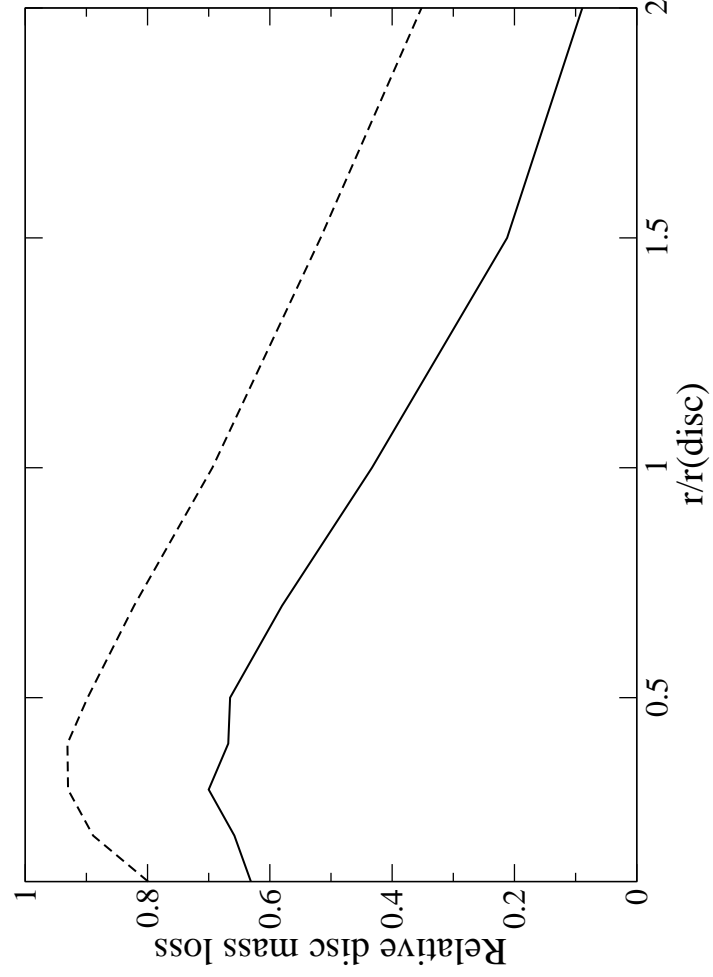


Fig. 5.— Relative disc mass loss, $\Delta M_d/M_d$, in parabolic encounters as a function of the relative periastron distance, exemplary for $M_2^* = 1 M_\odot$ (drawn line) and $M_2^* = 5 M_\odot$ (dashed line).

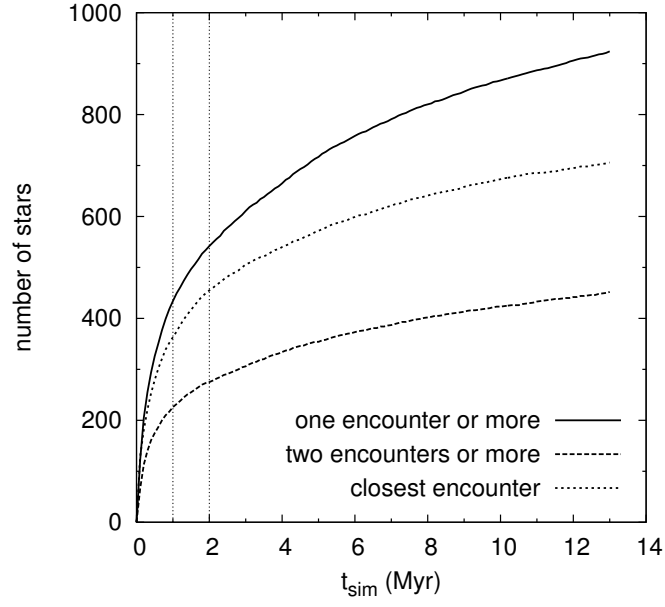


Fig. 6.— Number of stars that were subject to an encounter as a function of the simulation time. Comparison of three different encounter scenarios: all stars with at least one encounter, only stars with repeated encounters, and stars with the closest encounter only.

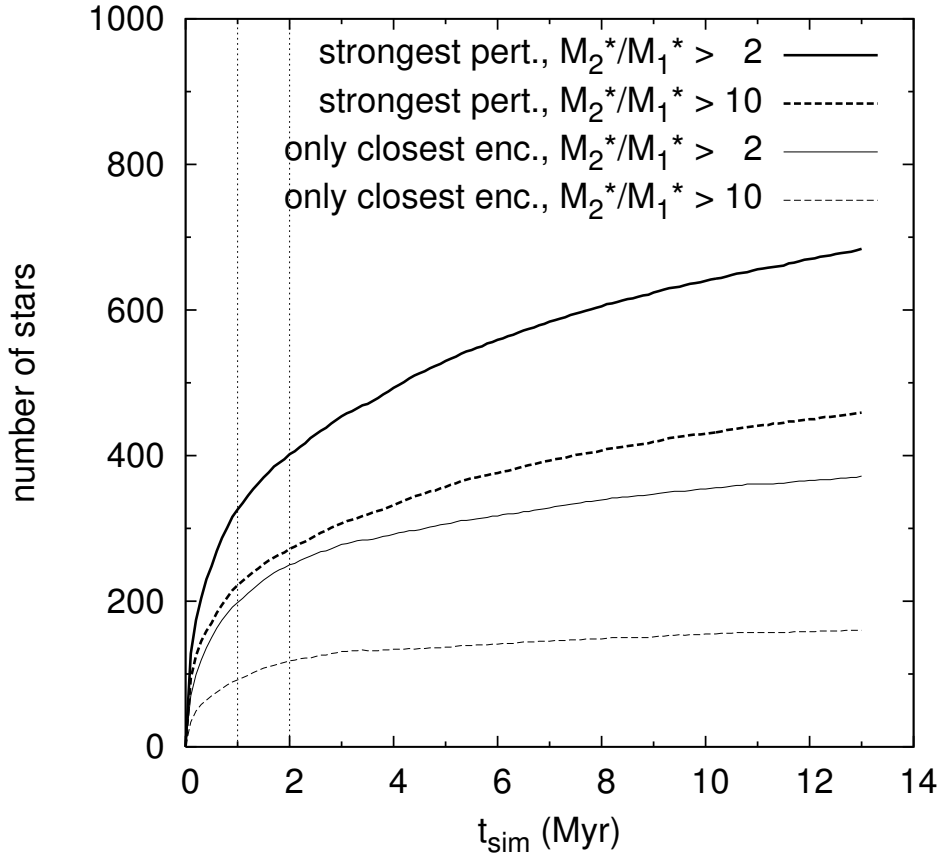


Fig. 7.— Number of stars that were subject to an encounter as a function of the simulation time. Comparison of the two different encounter definitions used in this work. The effect on the relative perturber mass is shown exemplary for $M_2^*/M_1^* > 2$ and $M_2^*/M_1^* > 10$, respectively.

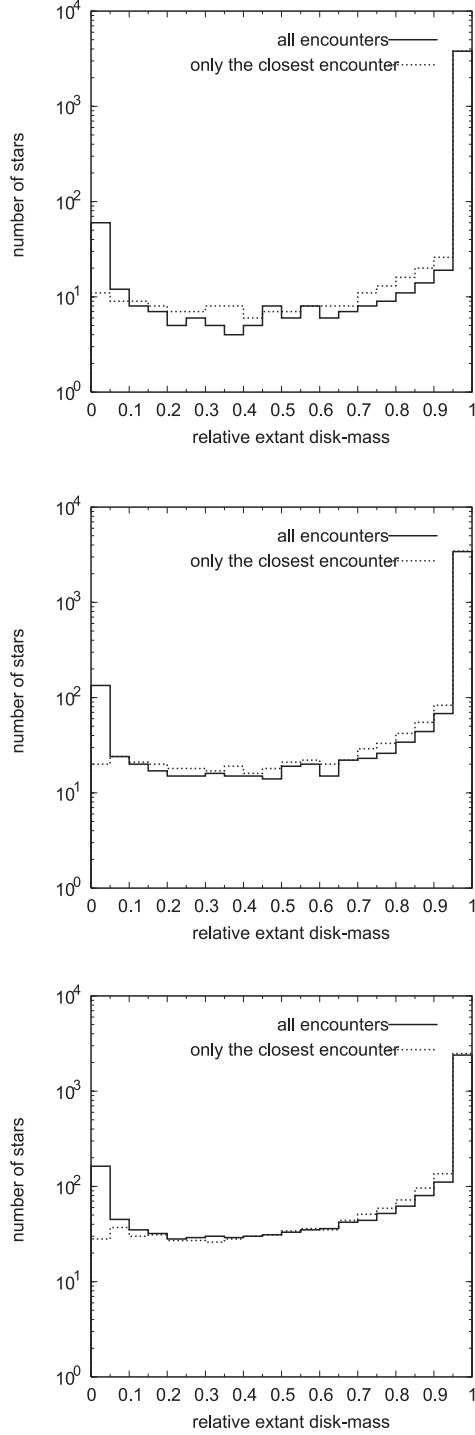


Fig. 8.— Distribution of the relative extant disc mass of all discs at three different times for model A. The output times correspond to shortly after the start of the simulation, $t_{\text{sim}} = 0.1$ Myr, to the lower limit on the mean age of the ONC, $t_{\text{sim}} = 1.0$ Myr, and to the end of the simulation at $t_{\text{sim}} = 13.0$ Myr.

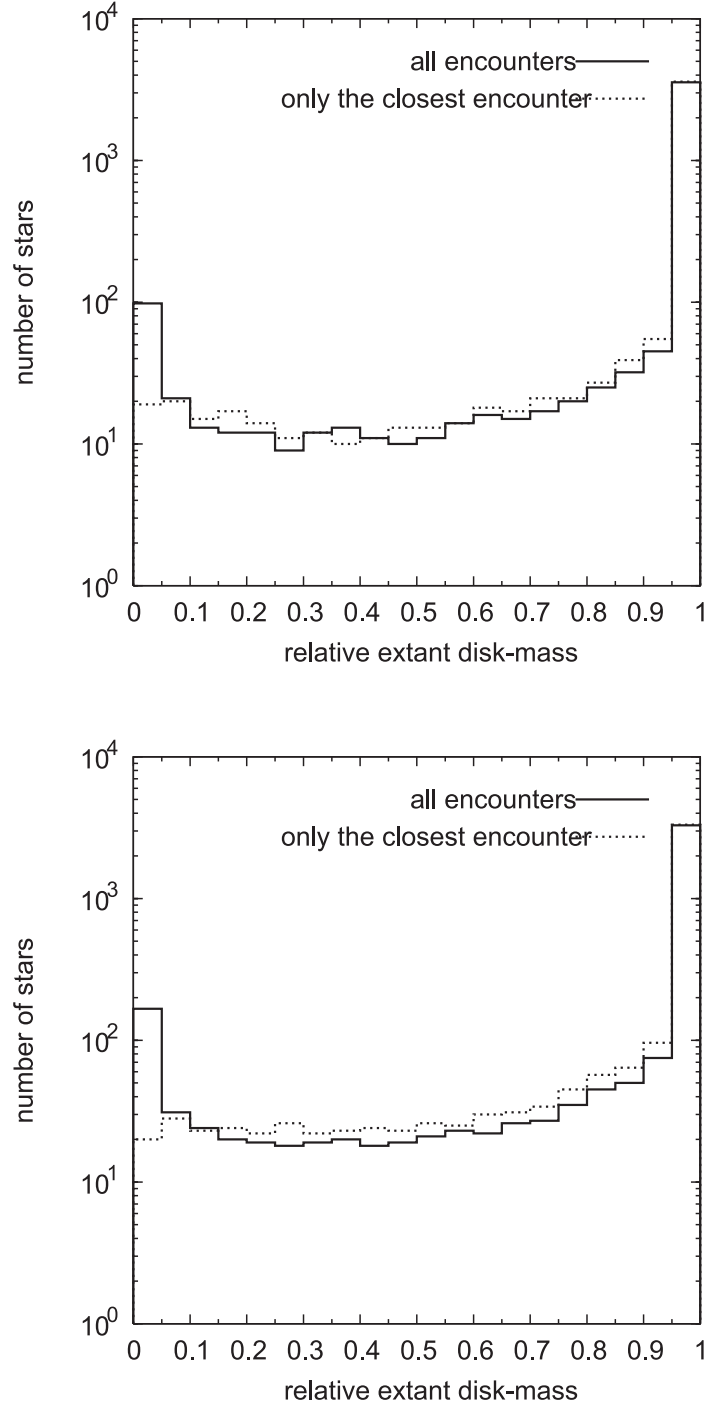


Fig. 9.— Distribution of the relative extant disc mass of all discs after $t_{\text{sim}} = 1$ Myr for two different standard disk sizes, $r_{\text{sd}} = 100$ AU (top) and $r_{\text{sd}} = 200$ AU (bottom), model A.

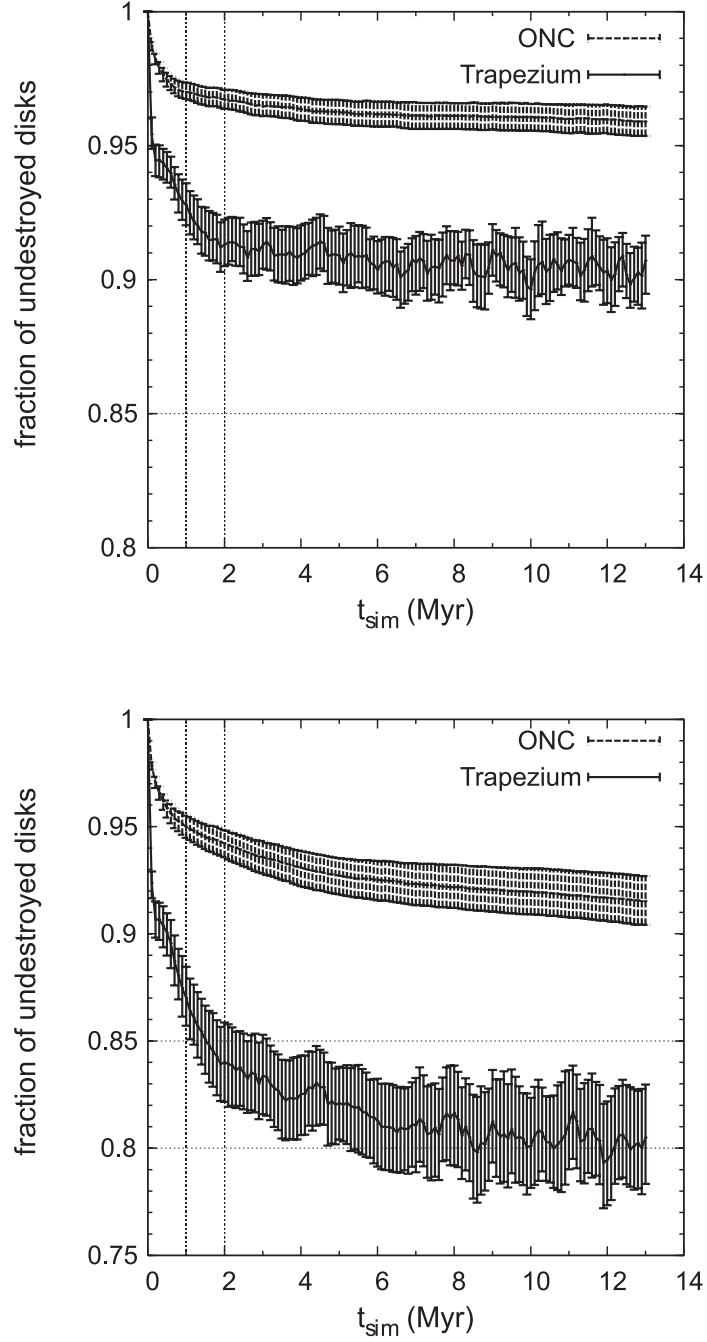


Fig. 10.— Fraction of un-destroyed discs (i.e. discs with at least 10% of their initial mass) in the ONC and the Trapezium cluster as a function of the simulation time, exemplary shown for $r_{sd} = 100$ AU (top) and $r_{sd} = 200$ AU (bottom), respectively, model A.

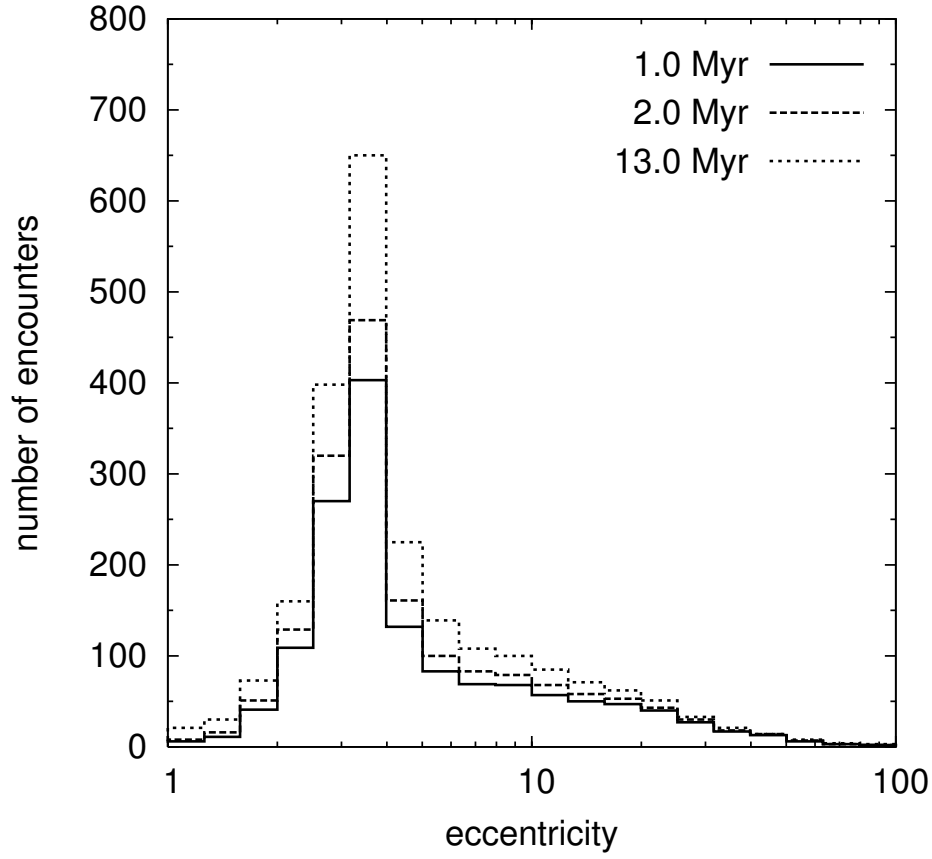


Fig. 11.— Histogram of the eccentricity of all encounters which have led to the disruption of discs (i.e. removal of more than 90% of the initial disc mass) within the specified simulation time, model A.

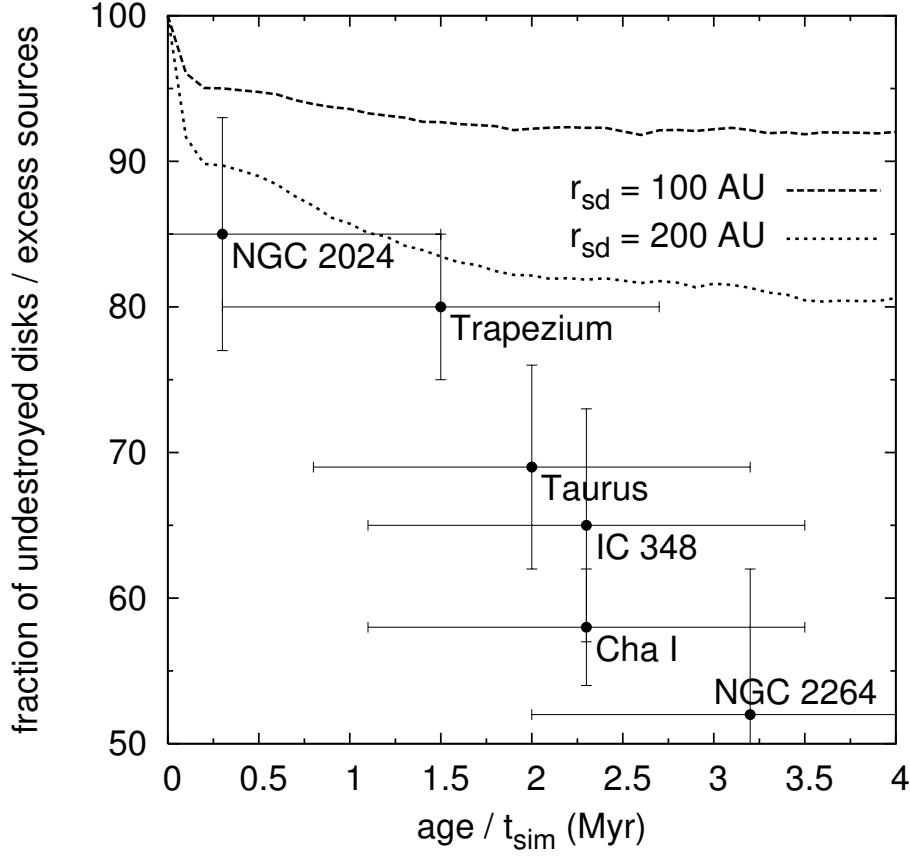


Fig. 12.— Fraction of un-destroyed discs (i.e. discs with at least 10% of their initial mass) in the Trapezium cluster for two different standard disc sizes, $r_{\text{sd}} = 100$ AU (dashed line) and $r_{\text{sd}} = 200$ AU (dotted line), model A (cf. Fig. 10). The simulation results are compared to the disc fraction of different star clusters, estimated from JHKL excess. The data were taken from Haisch, Lada & Lada (2001).

N	R_{ONC} [pc]	$\rho(r)$	ρ_{core} [pc ⁻³]	$\sigma_{3\text{D}}$ [km s ⁻¹]	$\xi(m)$	Q_{vir}	t_{ONC} [Myr]
≥ 4000	2.5	$\propto r^{-2}$	4.7×10^4	4.3 ± 0.5	KTG93	1.5?	≈ 2

Table 1: Main properties of the ONC.

Model	t_{out} [Myr]	Q_{vir}	N	N_{ONC}	R [pc]	R_{hm} [pc]	ρ_{core} [10 ⁴ pc ⁻³]	$\sigma_{3\text{D}}$ [km s ⁻¹]	t_{cross} [Myr]	t_{relax} [Myr]
A	0	0.50	4000	4000	1.10	0.55	27.6	4.11	0.4	24
	1	0.63	3999	3962	7.18	0.50	8.0	4.54		
	2	0.61	3998	3717	11.85	0.65	3.8	3.87		
A*	0	0.50	4000	4000	2.00	0.99	13.8	3.05	0.6	36
	1	0.60	4000	3902	4.99	0.87	3.6	3.58		
	2	0.62	3999	3647	11.46	0.89	1.5	3.44		
B	0	1.00	6000	6000	0.70	0.34	68.5	8.88	0.1	9
	1	1.11	5999	4986	9.33	1.07	4.4	5.79		
	2	1.36	5999	3762	20.22	1.40	2.1	5.52		
C	0	0.10	5000	4167	3.00	1.49	7.4	1.23	2.5	180
	1	0.33	5000	4201	3.24	1.45	10.6	2.49		
	2	0.46	5000	4316	5.00	1.34	8.0	3.06		
ONC	-	1.5 (?)	-	~ 4000	-	0.5–0.8	4.7	4.3	0.5	30

Table 2: Important quantities for the three most satisfying cluster models at different simulation times, compared to the ONC model, where t_{out} is the time of data output, Q_{vir} the virial ratio, N the total number of particles, N_{ONC} the number of particles inside 2.5 pc, R the total radius of cluster, R_{hm} the half-mass radius, ρ_{core} the stellar density of the inner core with radius 0.053 pc, $\sigma_{3\text{D}}$ the three-dimensional velocity dispersion, t_{cross} the crossing time and t_{relax} the relaxation time.

	500.0	90.0	50.0	20.0	9.0	5.0	4.0	3.0	2.0	1.5	1.0	0.5	0.3	0.1
0.1	0.930	0.899	0.879	0.890	0.862	0.799	0.737	0.713	0.694	0.680	0.631	0.599	0.423	0.167
0.2	0.950	0.940	0.929	0.932	0.919	0.889	0.868	0.850	0.829	0.787	0.658	0.561	0.396	0.161
0.3	0.979	0.983	0.982	0.965	0.950	0.930	0.913	0.876	0.831	0.786	0.700	0.528	0.349	0.155
0.4	0.987	0.987	0.987	0.981	0.965	0.931	0.911	0.886	0.819	0.764	0.668	0.489	0.291	0.140
0.5	0.991	0.989	0.987	0.979	0.941	0.898	0.880	0.846	0.799	0.740	0.665	0.475	0.255	0.138
0.7	0.990	0.986	0.983	0.941	0.883	0.822	0.798	0.752	0.690	0.655	0.580	0.432	0.225	0.119
1.0	0.989	0.969	0.938	0.873	0.781	0.694	0.660	0.615	0.550	0.500	0.433	0.284	0.175	0.090
1.5	0.980	0.898	0.846	0.742	0.613	0.517	0.475	0.419	0.340	0.293	0.212	0.118	0.084	0.024
2.0	0.955	0.827	0.759	0.619	0.469	0.352	0.308	0.248	0.175	0.125	0.089	0.037	0.019	0.000
2.5	0.915	0.751	0.664	0.493	0.336	0.218	0.181	0.139	0.089	0.052	0.023	0.001	0.000	0.000
3.0	0.877	0.671	0.570	0.385	0.224	0.114	0.089	0.054	0.026	0.013	0.000	0.000	0.000	0.000
3.5	0.831	0.601	0.487	0.286	0.132	0.060	0.040	0.019	0.001	0.000	0.000	0.000	0.000	0.000
4.0	0.793	0.523	0.397	0.209	0.085	0.018	0.006	0.000	0.000	0.000	0.000	0.000	0.000	0.000
4.5	0.740	0.461	0.318	0.133	0.033	0.002	0.000	0.000	0.000	0.000	0.000	0.000	0.000	0.000
5.0	0.705	0.386	0.255	0.097	0.013	0.000	0.000	0.000	0.000	0.000	0.000	0.000	0.000	0.0
5.5	0.654	0.310	0.190	0.048	0.000	0.000	0.000	0.000	0.000	0.000	0.000	0.000	0.0	0.0
6.0	0.618	0.252	0.156	0.029	0.000	0.000	0.000	0.000	0.000	0.000	0.0	0.0	0.0	0.0
6.5	0.575	0.211	0.104	0.012	0.000	0.000	0.000	0.000	0.000	0.0	0.0	0.0	0.0	0.0
7.0	0.537	0.156	0.087	0.001	0.000	0.000	0.000	0.000	0.000	0.0	0.0	0.0	0.0	0.0
7.5	0.492	0.132	0.047	0.000	0.000	0.000	0.0	0.0	0.0	0.0	0.0	0.0	0.0	0.0
8.0	0.459	0.117	0.034	0.000	0.000	0.000	0.0	0.0	0.0	0.0	0.0	0.0	0.0	0.0
8.5	0.418	0.079	0.011	0.000	0.000	0.0	0.0	0.0	0.0	0.0	0.0	0.0	0.0	0.0
9.0	0.373	0.071	0.005	0.000	0.000	0.0	0.0	0.0	0.0	0.0	0.0	0.0	0.0	0.0
9.5	0.340	0.038	0.001	0.000	0.0	0.0	0.0	0.0	0.0	0.0	0.0	0.0	0.0	0.0
10.0	0.291	0.026	0.000	0.000	0.0	0.0	0.0	0.0	0.0	0.0	0.0	0.0	0.0	0.0
10.5	0.265	0.010	0.000	0.000	0.0	0.0	0.0	0.0	0.0	0.0	0.0	0.0	0.0	0.0
11.0	0.229	0.005	0.000	0.000	0.0	0.0	0.0	0.0	0.0	0.0	0.0	0.0	0.0	0.0
11.5	0.216	0.000	0.000	0.0	0.0	0.0	0.0	0.0	0.0	0.0	0.0	0.0	0.0	0.0
12.0	0.176	0.000	0.000	0.0	0.0	0.0	0.0	0.0	0.0	0.0	0.0	0.0	0.0	0.0
12.5	0.168	0.000	0.000	0.0	0.0	0.0	0.0	0.0	0.0	0.0	0.0	0.0	0.0	0.0
13.0	0.134	0.000	0.000	0.0	0.0	0.0	0.0	0.0	0.0	0.0	0.0	0.0	0.0	0.0
13.5	0.130	0.000	0.000	0.0	0.0	0.0	0.0	0.0	0.0	0.0	0.0	0.0	0.0	0.0
14.0	0.098	0.000	0.000	0.0	0.0	0.0	0.0	0.0	0.0	0.0	0.0	0.0	0.0	0.0
14.5	0.098	0.000	0.000	0.0	0.0	0.0	0.0	0.0	0.0	0.0	0.0	0.0	0.0	0.0
15.0	0.069	0.000	0.000	0.0	0.0	0.0	0.0	0.0	0.0	0.0	0.0	0.0	0.0	0.0
15.5	0.070	0.000	0.0	0.0	0.0	0.0	0.0	0.0	0.0	0.0	0.0	0.0	0.0	0.0
16.0	0.071	0.000	0.0	0.0	0.0	0.0	0.0	0.0	0.0	0.0	0.0	0.0	0.0	0.0
16.5	0.047	0.000	0.0	0.0	0.0	0.0	0.0	0.0	0.0	0.0	0.0	0.0	0.0	0.0
17.0	0.042	0.000	0.0	0.0	0.0	0.0	0.0	0.0	0.0	0.0	0.0	0.0	0.0	0.0
17.5	0.023	0.0	0.0	0.0	0.0	0.0	0.0	0.0	0.0	0.0	0.0	0.0	0.0	0.0
18.0	0.021	0.0	0.0	0.0	0.0	0.0	0.0	0.0	0.0	0.0	0.0	0.0	0.0	0.0
18.5	0.010	0.0	0.0	0.0	0.0	0.0	0.0	0.0	0.0	0.0	0.0	0.0	0.0	0.0
19.0	0.008	0.0	0.0	0.0	0.0	0.0	0.0	0.0	0.0	0.0	0.0	0.0	0.0	0.0
19.5	0.002	0.0	0.0	0.0	0.0	0.0	0.0	0.0	0.0	0.0	0.0	0.0	0.0	0.0
20.0	0.001	0.0	0.0	0.0	0.0	0.0	0.0	0.0	0.0	0.0	0.0	0.0	0.0	0.0

Table 3: Table of relative disk mass losses $\Delta M_d/M_d$ for all simulated configurations of parabolic ($e = 1$) star-disc encounters. The first row contains the relative perturber masses M_2^*/M_1^* , the first column contains the relative periastra r_p/r_d . Results from simulations are denoted by four digits, the values “0.0” were edited manually.

